Structural Evolutions of Nanostructured CoAl Intermetallic Compound during Mechanical Alloying and Subsequent Heat Treatment

F. Karimzadeh,*, M.H. Enayati,†, S.N. Hosseini,‡

Department of Materials Engineering, Isfahan University of Technology, 84156-83111, Isfahan, Iran

Nanostructured B2-CoAl has been successfully synthesized directly by MA of nominal composition of Co50Al50. The CoAl phase was found to be formed in an ordered structure via a gradual reaction which completed in less than 10 h. However, further milling up to 45 h led to disordering of the CoAl with a relatively constant long-range order parameter of 0.82. Lattice parameter measurements showed that disordering of CoAl was caused by triple defect mechanism. The results of isothermal annealing showed that the grains grew after isothermal annealing up to 0.7 Tm but still remained below 100 nm. The grain growth behavior was well described by the parabolic kinetics equation. The grain growth exponent remained constant above 873 K offering that grain growth mechanism does not change at high temperatures. The grain growth exponents and activation energies offered the mechanism of diffusing Co and Al atoms in the two separate sublattices at high temperatures. The equation $D^4 - D_0^4 = 6 \times 10^{13} \ \exp\left[-175/RT\right] \ t$ was suggested to describe the grain-growth kinetics of nano-crystalline CoAl during isothermal annealing at temperatures above 0.5T$_m$ (873 K).

Keywords: Intermetallic Compounds, CoAl, Nanostructures, Grain Growth, Mechanical Alloying.

PACS numbers: 71.20.Lp, 81.20.Ev

1. INTRODUCTION

The intermetallic compound CoAl with B2 structure is a promising material for many high-temperature applications due to its melting temperature (1648°C), density (6.086 Mg/m3), moderate oxidation resistance and thermal conductivity [1]. A common feature of the B2 type CoAl phase is that it has a broad composition range and the highly ordered bcc structure of the CoAl phase is maintained up to its melting temperature [1-2]. It is known that the physical and mechanical properties of brittle intermetallics can significantly alter by controlling the microstructure in the nanoscale. Nanocrystalline materials can exhibit improved ductility and fracture toughness. Non-equilibrium processing techniques such as mechanical alloying/milling can produce metastable microstructure with the grain size reduced to nanoscale and therefore, this processing technique has been extensively employed to synthesize intermetallics. These materials can be used as, for example, dispersoids, coatings, high specific surface area powders, functional nanodevices and engine parts [3-4].

In general, MA of elemental metal blend may lead to the formation of the intermetallic, solid solution or amorphous phases [5]. In Co-Al binary system, it is reported that MA of Co50-Al50 led to the formation of CoAl intermetallic compound [6]. Although it has been reported that prolonged mechanical milling (MM) of fully ordered CoAl produced by other techniques than MA leads to partly disordering [7], no report exists on ordering-disordering behavior of CoAl during MA.

Grain growth in polycrystalline materials, in general, occurs to decrease the free energy of the system by decreasing the total grain boundary energy. In nano-crystalline (nc) materials, high amount of grain boundary leads to a significant fraction of high energy and provides a strong driving force for grain growth. Since the unique properties of these materials are closely related to the fine grain size and the large volume fraction of grain boundaries, it is of vital importance to maintain the microstructure at a nanometeric scale during consolidation or service as structural components at elevated temperatures [8-11]. With this regard, many studies have been focused on the grain growth behavior of nc materials (e.g., see References [12-14]).

Although different models were proposed grain growth models for nc materials taking into accounts of the impurities and solute drags, it was reported that some nc materials still obeyed the parabolic kinetic equation of grain growth for isothermal annealing in the form [15-17]

$$D^n - D_0^n = Kt \qquad (1)$$

where D, D_0 and n are the mean grain size at time t, mean initial grain size, and the grain-growth exponent, respectively. K is a constant that satisfies the following equation [15-17]

$$K = K_0 \exp(-Q/RT) \qquad (2)$$

Where Q is the activation energy required for grain growth and K_0, R and T are constant, gas constant and temperature, respectively. Eqs. (1) and (2) can be rewritten as [17]

$$D^n - D_0^n = K_0 \ \exp\left[-Q/RT\right] \ t \qquad (3)$$

* Karimzadeh_f@cc.iut.ac.ir
† ena78@cc.iut.ac.ir
‡ golenarges63@yahoo.com

In addition, the rate of grain growth, dD/dt , can be derived as

$$\log\left[dD(t)/dt \right] = -(n-1)\log D(t) + \log K - \log n \quad (4)$$

The relationship between $\log dD(t)/dt$ and $\log D(t)$ gives the values of n and K. Also, the activation energy Q can be obtained from Equation (3) by plotting $\log\left[\left(D^n - D_0^n \right)/t \right]$ as a function of $1/T$. A variety of n values has been reported for various systems and the n value can be a useful factor to describe the difference in growth mechanism between the different systems [16]. So, the aim of the present work is mainly to investigate MA of the Co50-Al50 mixture and to investigate thermal stability and grain growth kinetics of the nanostructured CoAl synthesized by MA.

2. EXPERIMENTAL PROCEDURE

MA of the Co-50at.%Al powder blend was carried out at ambient temperature in a planetary high energy ball mill, using hardened chromium steel vial and balls. No process control agent (PCA) was used. The related parameters for the MA are presented in Table 1. Isothermal annealing was performed to investigate the grain growth kinetics of milled powders. Powder samples were sealed and then annealed in a conventional tube furnace. The annealing process parameters are displayed in Table 1. X-ray diffraction (XRD) technique by a Philips X'PERT MPD diffractometer (Cu Kα radiation: λ = 0.154 nm at 20 kV and 30 mA) was used to characterize the phase composition and structural changes of the powders. The Williamson–Hall formula was used to estimate the grain size and internal strain using broadening of XRD peaks [18].

Table 1 – Parameters for MA and heat treatment.

Parameters	Value
Rotation speed (r/min)	600
Ball to powder weight ratio	15:1
Ball milling time (h)	1, 3, 6, 10, 25 and 45
Protective atmosphere	Ar
Annealing temperature (K)	873, 973, 1073 and 1173
Holding time (h)	0.5, 1, 1.5
Cooling mode	Cooling in air

3. RESULTS AND DISCUSSION

3.1 MA of Co-50 at%.Al

Fig .1 shows XRD traces for Co50Al50 powders as-received and after different MA times. During MA the sharp crystalline diffraction peaks of the as-received powder broadened progressively with increasing processing time associated with accumulated internal strain and refinement of grain size. The Co and Al grain size and lattice strain after 1 and 3 h MA, estimated from broadening of XRD peaks using Williamson–Hall formula [18], were presented in Table 2.
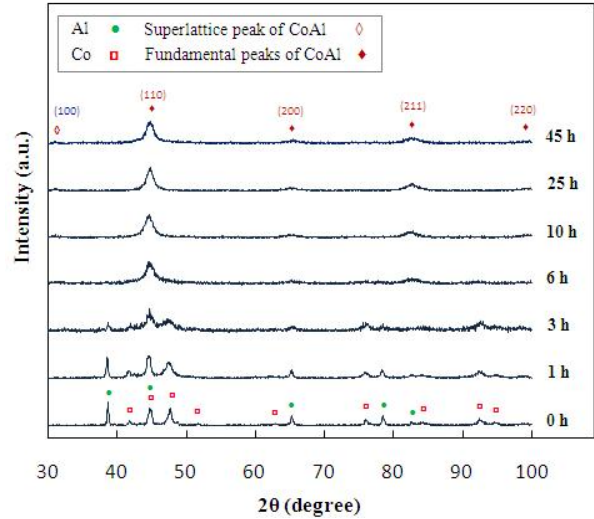

Fig. 1 – The XRD patterns of the Co50-Al50 powder mixture at different MA time.

It can be seen that after 3 h MA, the final grain size of Co is smaller and its lattice strain is greater than that for Al. Although the initial grain size was smaller for Co, this might be due to their different crystal structures. Cobalt (with hcp structure) is a material with low stacking fault energy in which dislocation slip is the dominant deformation mechanism. But it is reported [19] that the nanocrystalline cobalt deforms predominantly by mechanical twinning. Dislocation slip in the nanocrystalline cobalt is hindered by the small grain size and twinning (in despite of higher activation energy requirement) proceeds. Although the classical twinning process based on the pole mechanism would be difficult to apply for very small grain sizes, a recent molecular dynamics simulation study [20] showed that, at high stress levels, both heterogeneous (starting at grain boundaries) and homogenous nucleation of twins can occur for materials with grain sizes less than 50 nm. Homogeneous nucleation took place in the grain interiors and involved the overlap of stacking faults of dissociated dislocations. So, the material exhibits an unusually faulted microstructure [19]. However, in the case of nanocrystalline Al, the higher stacking fault energy for Al (200 mJ/m²) [21] in comparison with cobalt (31 mJ/m²)[19] and the tendency of Al (with fcc structure) to slip will make deformation based on twinning more difficult.

Table 2 – Grain size and lattice strain of Co and Al at different MA times.

MA time	Co		Al	
(h)	d (nm)	ε (%)	d (nm)	ε (%)
1	23	0.46	55	0.35
3	9	0.63	20	0.53

From 1 to 3 h MA, the powder particles were agglomerated and large amount of powders were stuck to the surfaces of the container and balls. Further milling resulted in the release of coated Co and Al and appearance of CoAl peaks. Transformation of elemental Co and Al powder mixture to the CoAl intermetallic phase was completed after 10h MA. The detection of superlattice

reflection (100) indicates that the B2-CoAl phase has an ordered structure. The long range order parameter (S) was calculated considering the (100) superlattice reflection and (110) fundamental reflection of cubic B2 structure formed by MA using the following formula [22]:

$$S = \sqrt{\frac{I_{100}/I_{110\ obs}}{I_{100}/I_{110\ std}}} \qquad (5)$$

Where subscripts "obs" and "std" stand for observed and Standard ratios of the intensities of the mentioned diffracting atomic planes. Here standard ratio refers to that for a completely ordered structure.

The S parameter, grain size and lattice strain of the B2-CoAl calculated for different MA times, are presented in Table 3.

Table 3 – Structural characteristics of the CoAl phase at different MA times.

MA time (h)	d (nm)	ε (%)	Lattice parameter (A°)	S
6	6	0.75	2.862	1
10	7	0.36	2.862	1
25	7	1.41	2.857	0.82
45	6	1.63	2.856	0.82

As can be seen the S value is equal to 1 during 6 to 10 h milling suggests that formed B2-CoAl is fully ordered. The S value decreases and reaches a constant value of about 0.82 after long milling periods. The grain size of the formed CoAl is about 6 nm that remains approximately constant with further milling. These results are in agreement with the general observation that up-on ball milling, for most intermetallic compounds a refinement of the internal grain size is observed to typically 5 to 20 nm together with an increase of atomic level strains typically between 0.7 and 2.5%[23] (see Table 3). The minimum grain size achievable by milling is determined by the competition between the plastic deformation via dislocation motion and the recovery and recrystallization behavior of the material. This balance gives a lower bound for the grain size of the material. Besides, a number of process variables (such as method to estimate the grain size, milling intensity, milling temperature, alloying effects, contamination, etc.) can influence the minimum achievable grain size [7].

In some instances, ordered intermetallics have been found to be formed directly on MA, although it is particularly true in Al-transition metal systems [7]. At the early stage of milling, nanometric grain sizes and high defect densities produced by MA accelerate the Co–Al interdiffusion process at room temperature. Therefore, CoAl phase starts to form after 6 h MA. The heat released from this reaction is consumed to release stored energy, which was incorporated during ball milling. So, the lattice strain of the B2-CoAl decreases from 0.75 to 0.36%. After completion of CoAl formation, the lattice strain increases again and S value decreases on further milling due to severe plastic deformation. It is reported that disordering in B2-CoAl compound occurs with triple defect mechanism that results in reducing the lattice parameter [3,7,24-25]. So, triple defects formation can be responsible for decrease of lattice parameter from 2.862 to 2.856 Ao.

3.2   Heat Treatment

In order to investigate grain growth, annealing of the as-milled powder was performed at different temperatures and durations. The corresponding XRD patterns are shown in Fig. 2. The grain size of nano-crystalline CoAl, calculated from XRD patterns, are plotted as a function of annealing time (see Fig. 3).
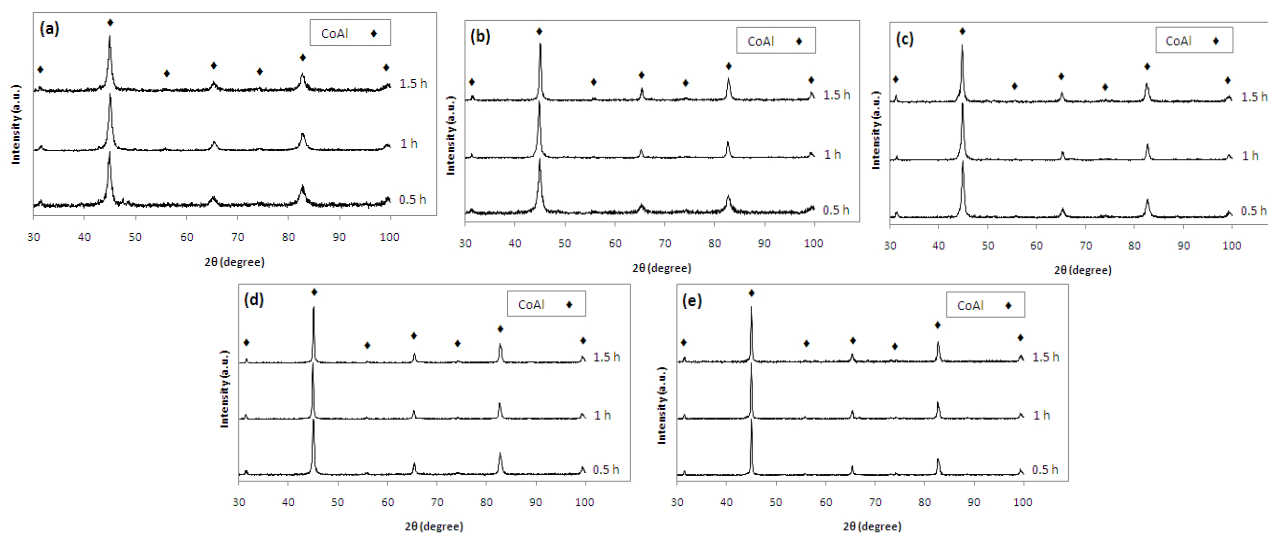

Fig. 2 – XRD patterns of the isothermally annealed powders at a)873, b)973, c)1073, d)1173 and e)1273 K for 0.5, 1 and 1.5 h
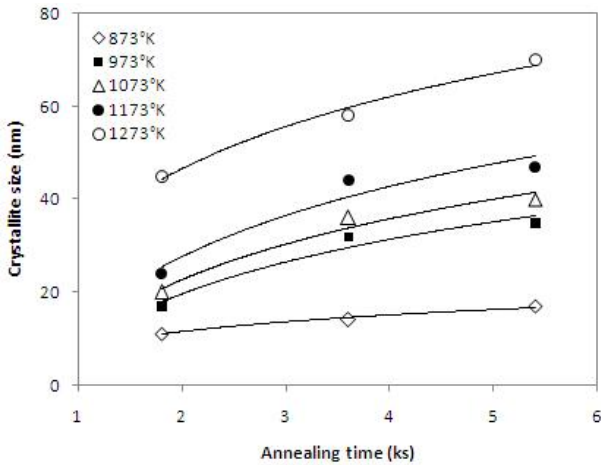
Fig. 3 – Grain size of the CoAl as a function of annealing time for different temperatures

As it is expected, the grain size increases with increasing the temperature. The grain size does not hugely vary with annealing time especially at T≥973 K. The grain size increases rapidly first and then almost evenly at the longer annealing times. This can be interpreted as a result of the decrease in the interfacial energy during grain growth [7]. The plots of $\log dD(t)/dt$ versus $\log(D)$ (Fig. 4) were obtained by fitting the data to Eq. (4) using a non-linear fitting route. The value of n is about 3 for 873 K while reaches to a constant value of 4 at higher temperatures (T/Tm≥0.5). It is reported that n value depends on grain growth mechanism [15-16]. So, it is appeared that grain growth mechanism of the nano-crystalline CoAl compound is the same at the temperature range of 973-1273 K. Normal grain growth of pure materials ($n = 2$) is controlled by curvature-driven migration of grain boundaries. When $n = 3$, grain growth process is governed by volume diffusion. If $n = 4$, the stochastic jumping of atoms across the grain boundaries is predominant. As observed experimentally, the n values usually ranges from 2 to >5 for conventional pure metals as well as some of the MAed intermetallic compounds e.g. nano-crystalline Fe with the n value in the range of 3-11 [9-10, 15, 17]. In conventional materials, the value of n is dependent on both mobility and energy of the grain boundaries. Wang et al. [15, 17] reported that for nano-Fe, similar to coarse-grained Fe, n decreases toward 2 as T/Tm increases to ≈0.6. The growth exponent n obtained in this work indicates that nano-CoAl shows high resistance against grain growth compared to nano-Fe or conventional coarse-grained Fe. In addition, this value offers that the grain growth mechanism of the nanostructured CoAl at temperatures above 873K (T/Tm≈0.5) can be the random jump of atoms across the grain boundaries. Considering the fact that nanostructured CoAl consists of nanometer-sized grains and has a large volume fraction of grain boundaries, grain growth through atom diffusion in these boundaries is expected much easier than that through conventional lattice diffusion.

By plotting $\log\left[D^n - D_0^n \ / t \right]$ versus $1/T$ and fitting a straight line to the data points (Fig. 5), the activation energy for grain growth of nano-crystalline CoAl

compound was calculated to be 175±20 kJ/mol. This value of Q is quite smaller than the activation energy of both interdiffusion in conventional CoAl (≈432 kJ/mol) [2] and self-diffusion of Co in conventional CoAl (≈416 kJ/mol) [26]. But, it is approximately close to the activation energy for diffusion of Co in Al (83 Kj/mol) [27] and also the activation energy of Al volume self-diffusion (144 kJ/mol) [10]. As mentioned before, the CoAl phase has a disordered structure with the triple defects formation mechanism in which CoAl structure is maintained by remaining Al atoms on their own sublattices. So, it can be said that the grain growth in disordered CoAl phase is accomplished by diffusing Co and Al atoms in the two separate Al and Co sublattices.
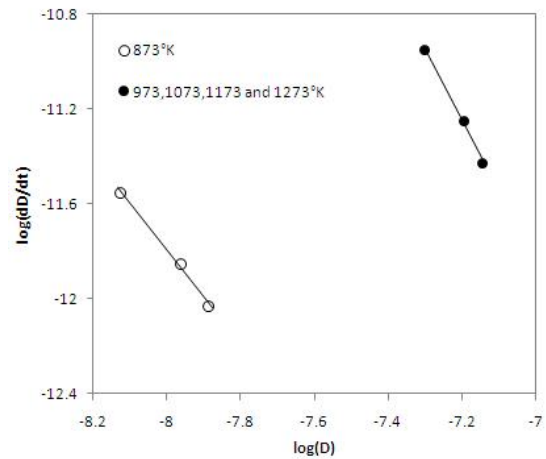

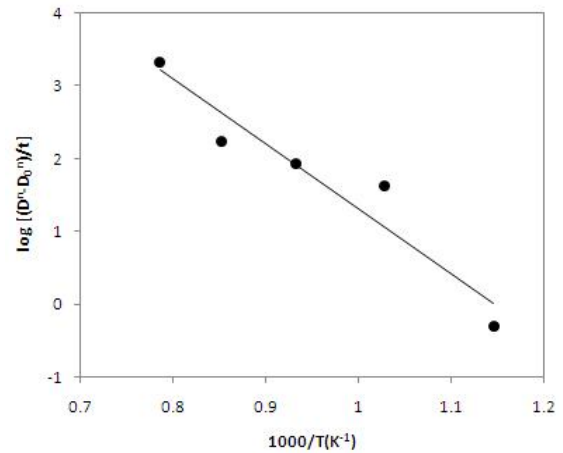**Fig. 4** – Plots of $\log dD(t)/dt$ versus $\log(D)$ for CoAl phase at different annealing temperatures

Fig. 5 – Plot of $\log\left[D^n - D_0^n \ / t \right]$ against $1000/T$ for CoAl grains

Consequently, the grain-growth kinetics of nano-crystalline CoAl under isothermal annealing at temperatures above 873 K can be well described using

$$D^4 - D_0^4 = 6 \times 10^{13} \ \exp\left[-175 \ / \ RT \right] t \qquad (6)$$

Eq. (6) provides the means by which the grain size of nano-crystalline CoAl can be controlled by simply governing the annealing temperature and time

REFERENCES

1. Y. Takano, *J. Am. Ceram. Soc.* **84**, 2445 (2001).
2. R. Nakamura, K. Takasawa, Y. Yamazaki, Y. Iijima, *Intermetallics* **10**, 195 (2002).
3. H. Bakker, G.F. Zhou and H. Yang, *Progr. Mater. Sci.* **39**, 159 (1995).
4. N.K. Mukhopadhyay, D. Mukherjee, S. Dutta, R. Manna, D.H. Kim, I. Manna, *J. Alloys Compd.* **457**, 177 (2008).
5. P. Nandi, P.M.G. Nambissan and I. Manna, *J. Alloys Compd.* **377**, 179 (2004).
6. V.K. Portnoi, K.V. Tretyakov, V.I. Fadeeva, *Inorg. Mater.* **40**, 937 (2004).
7. C. Suryanarayana, *J. Prog. Mater. Sci.* **46**, 1 (2001).
8. J. Lee, F. Zhou, K.H. Chung, N.J. Kim, E.J. Lavernia, *Metall. Mater. Trans* **32**(A), 3109 (2001).
9. M. Kazeminezhad, *Bull. Mater. Sci.* **32**(1), 19 (2009).
10. F. Liu, G. Yang, H. Wang, Z. Chen, Y. Zhou, *Thermochim. Acta* **443**, 212 (2006).
11. K.W. Liu, F. Mucklich, *Acta Mater.* **49**, 395 (2001).
12. M. Lewandowska, K.J. Kurzydlowski, *Materials Characterization* **55**, 395 (2005).
13. S. Sivasankaran, K. Sivaprasad, R. Narayanasamy, P.V. Satyanarayana, *Materials Characterization* **62**, 661 (2011).
14. Z. Horita, D.J. Smith, M. Furukawa, M. Nemoto, R.Z. Valiev, T.G. Langdon, *Materials Characterization* **37**, 285 (1996).
15. M.A. Thein, L. Lu, M.O. Lai, *Compos. Sci. Tech.* **66**, 531 (2006).
16. M. Kambara, K. Uenishi, K.F. Kobayashi, *J. Mater. Sci.* **35**, 2897 (2000).
17. R. Ren, Y.C. Wu, W.M. Tang, F.T. Wang, T.G. Wang, Z.X. Zheng, *Trans. Nonferrous Met. Soc. China* **18**, 66 (2008).
18. G.K. Williamson, W.H. Hall, *Acta Met.* **1**, 22 (1953).
19. A.A. Karimpoor, U. Erb, K.T. Aust, G. Palumbo, *Scripta Mater.* **49**, 651 (2003).
20. V. Yamakov, D. Wolf, S.R. Phillpot, H. Gleiter, *Scripta Mater.* **50**, 5005 (2002).
21. G.E. Dieter, Mechanical metallurgy, 3rd Ed., McGraw-Hill (1976).
22. T. Mousavi, F. Karimzadeh, M.H. Abbasi, *Mater. Sci. Eng. A* **487**, 46 (2008).
23. J.R. Groza, J.F. Shackelford, E.J. Lavernia, M.T. Powers, *Materials processing hand book* (Taylor and Francis: 2007).
24. H. Mehrer, *Diffusion in solids: fundamentals, methods, materials, diffusion controlled processes* (Springer: 2007).
25. H. Bakker, I.W. Modder, M.J. Kuin, *Inrermerollics* **5**, 535 (1997).
26. R. Nakamura, Y. Iijima, *Intermetallics* **13**, 163 (2005).
27. R.P. Agarwal, S.P. Murarka, M.S. Anand, *Acta Met.* **12**, 871 (1964).